

Main Group Tellurium Heterocycles Anchored by a $P_2^V N_2$ Scaffold and Their Sulfur/Selenium Analogues

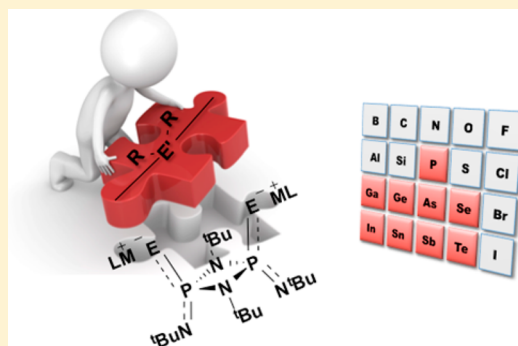
Andreas Nordheider,^{†,‡} Katharina Hüll,[†] Joanna K. D. Prentis,[†] Kasun S. Athukorala Arachchige,[†] Alexandra M. Z. Slawin,[†] J. Derek Woollins,[†] and Tristram Chivers^{*,‡}

[†]EaStCHEM School of Chemistry, University of St. Andrews, St. Andrews, Fife KY16 9ST, U.K.

[‡]Department of Chemistry, University of Calgary, Calgary, Alberta, Canada T2N 1N4

Supporting Information

ABSTRACT: A comprehensive investigation of reactions of alkali-metal derivatives of the ditelluro dianion $[TeP^V(N^tBu)(\mu-N^tBu)]_2^{2-}$ (L^{2-} , $E = Te$) with p-block element halides produced a series of novel heterocycles incorporating $P_2^V N_2$ rings, tellurium, and group 13–16 elements. The dianion engages in Te,Te'-chelation to the metal center in Ph_2Ge and R_2Sn ($R = ^tBu, ^nBu, Ph$) derivatives; similar behavior was noted for group 14 derivatives of L^{2-} ($E = S, Se$). In the case of group 13 trihalides MCl_3 ($M = Ga, In$), neutral spirocyclic complexes $(L)M[N^tBu(Te)P^V(\mu-N^tBu)_2P^{III}N(H)^tBu]$ ($M = Ga, In$) comprised of a Te,Te'-chelated ligand L^{2-} and a N,Te-bonded ligand resulting from loss of Te and monoprotection were obtained. In reactions with $RPCL_2$ ($R = ^tBu, Ad, ^iPr_2N$) a significant difference was observed between Se- and S-containing systems. In the former case, Se,Se'-chelated derivatives were formed in high yields, whereas the N,S-chelated isomers predominated for sulfur. All complexes were characterized by multinuclear ($^1H, ^{31}P, ^{77}Se, ^{119}Sn, \text{ and } ^{125}Te$) NMR spectroscopy; this technique was especially useful in the analysis of the mixture of $(L)(Se)$ and $(L)(SeSe)$ obtained from the reaction of Se_2Cl_2 with L^{2-} ($E = Te$). Single-crystal X-ray structures were obtained for the spirocyclic In complex (**9**), $(L)GePh_2$ ($E = Te, \text{ 10}$), $(L)Sn^tBu_2$ ($E = Te, \text{ 12a}$); $E = Se, \text{ 12aSe}, E = S, \text{ 12aS}$) and $(L)(\mu-SeSe)$ ($E = Te, \text{ 16}$).



INTRODUCTION

Cyclodiphosphazanes, for example, $[CIP^{III}(\mu-NR)]_2$, are saturated, four-membered $P^{III}_2N_2$ rings that continue to attract interest from the inorganic chemistry community.^{1,2} In recent studies they have been used creatively as building blocks in the synthesis of macrocycles with amido (NH) or chalcogenido (O, S, Se) linkers,³ as well as those that incorporate coinage metals coordinated to the phosphorus(III) centers.⁴ A fascinating recent example is afforded by the Cu_4X_4 clusters linked by P_2N_2 rings that resemble a sodalite framework.⁵ In some cases these macrocycles are able to encapsulate halide⁶ or perchlorate anions.⁷

The P^{III}/P^{III} systems with terminal alkylamido groups, for example, $[^tBuN(H)P^{III}(\mu-N^tBu)]_2$, are readily oxidized by sulfur or selenium.⁸ Subsequent double deprotonation of the resulting P^V/P^V dichalcogenides $[^tBuN(H)(E)\{P^V(\mu-N^tBu)\}]_2$ produces ambidentate dianions of the type L^{2-} ($E = S, Se$), which coordinate to alkali metals in either a “top and bottom” fashion (N,N' and E,E') for the sodium and potassium derivatives **1** and **2** (Chart 1) or in a side-on mode (bis-N,E) for the lithium analogues;^{9,10} dimethylaluminum derivatives also adopt bis-N,E chelation.¹¹ Monodeprotonation of $[^tBuN(H)(E)\{P^V(\mu-N^tBu)\}]_2$ ($E = S, Se$) generates the corresponding monoanions, which attach to Li^+ in a mono-N,E bonding

arrangement.¹⁰ Recently, we have shown that the two-electron oxidation of the dianions L^{2-} ($E = S, Se$) produces 15-membered macrocycles in which a planar P_6E_6 platform is stabilized by perpendicular $P_2^V N_2$ rings.¹² In the case of $E = Se$ this oxidation also gives rise to the bridging tetraselenide $[^tBuN\{P^V(\mu-N^tBu)\}]_2(\mu-SeSeSeSe)$ (**3**) (Chart 1), which is more conveniently prepared by metathesis of **2** with Se_2Cl_2 .¹²

The synthesis of the ditelluro dianion L^{2-} ($E = Te$) requires a different approach because elemental tellurium does not oxidize both P^{III} centers in $[^tBuN(H)P^{III}(\mu-N^tBu)]_2$. However, if the double deprotonation of this neutral precursor is performed first,¹³ the P^{III} centers in the resulting dianion become more nucleophilic and telluration proceeds smoothly to give L^{2-} ($E = Te$) as either dilithium or disodium derivatives, **4** or **5** (Chart 2), respectively.^{14,15a} As in the case of the dithio analogue L^{2-} ($E = S$), the smaller Li^+ ions in **4** adopt a different coordination mode (Te,Te' and N,Te)¹⁴ compared to that found for Na^+ in **5** (Te,Te' and N,N').^{15a}

In contrast to the formation of trimeric macrocycles from the oxidation of alkali-metal derivatives **1** and **2** (vide supra),¹² the treatment of **4** with I_2 produces the cyclic tritelluride

Received: January 26, 2015

Published: February 26, 2015

Chart 1

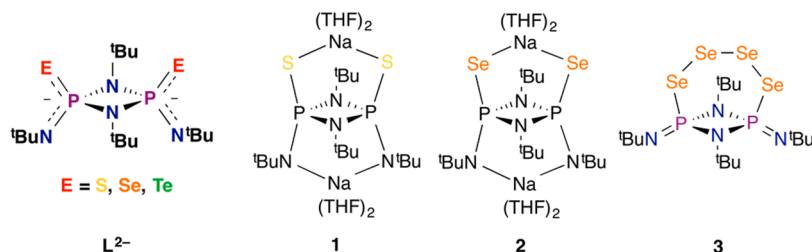
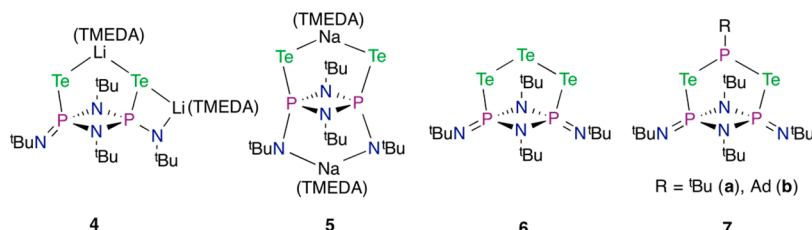


Chart 2



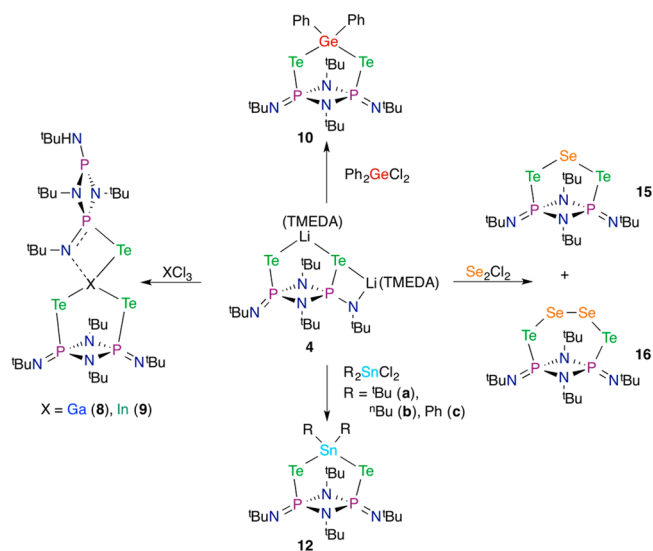
$[{}^tBuN\{P^V(\mu-N{}^tBu)\}]_2(\mu-TeTeTe)$ (**6**, Chart 2), which is obtained in higher yield by metathesis of **5** with $TeCl_2 \cdot TMTU$ ($TMTU = \text{tetramethylthiourea}$).^{15a} Furthermore, metathesis of **4** with $RPCl_2$ ($R = {}^tBu, Ad$) generates the P_2N_2 -supported heterocycles **7a,b** (Chart 2), which were among the first examples of structurally characterized phosphorus(III)–tellurium ring systems.^{15b} The unusual ditellurido-bridged P_2N_2 ring $[(\mu-N\text{Ter})P]_2(\mu-TeTe)$ has also been reported recently.¹⁶

These preliminary results suggest that the P_2N_2 scaffold plays an influential role in the stabilization of heterocycles that incorporate tellurium and another p-block element. To determine the scope and limitations of the ditelluro dianion L^{2-} ($E = Te$) as a reagent for the synthesis of such heterocycles, we performed a comprehensive investigation of the reactions of **4** and **5** with a variety of group 13, 14, 15, and 16 halides, specifically, MCl_3 ($M = Ga, In$), R_2MCl_2 ($M = Ge, R = Ph$; $M = Sn, R = {}^tBu, {}^nBu, Ph$), $RMCl_2$ ($M = As, R = Et$; $M = Sb, R = Ph$), and Se_2Cl_2 . For comparison, we conducted the reactions of the dithio and diseleno reagents **1** and **2**, respectively, with group 14 dihalides and $RPCl_2$ ($R = {}^tBu, Ad, {}^iPr_2N$). The products of these metatheses were characterized by CHN analyses, high-resolution mass spectra, and, in solution, by multinuclear NMR spectroscopy (${}^1H, {}^{31}P, {}^{77}Se, {}^{119}Sn, \text{ and } {}^{125}Te$). Solid-state structures of the spirocyclic In complex (**9**), $(L)GePh_2$ ($E = Te, \mathbf{10}$), $(L)Sn{}^tBu_2$ ($E = Te, \mathbf{12a}$; $E = Se, \mathbf{12aSe}$, $E = S, \mathbf{12aS}$), and $(L)(\mu-SeSe)$ ($E = Te, \mathbf{16}$) were determined by single-crystal X-ray crystallography.

RESULTS AND DISCUSSION

Synthesis, NMR Spectra, and Crystal Structure of Group 13 Complexes. The reactions of **4** and **5** with group 13–16 halides were performed in toluene at $-78\text{ }^\circ\text{C}$, followed by warming to room temperature. The crude products were generally recrystallized from *n*-hexane at $-40\text{ }^\circ\text{C}$, and X-ray structural determinations were performed when suitable crystals were obtained. In other cases the identity of the products was based on high-resolution mass spectra and multinuclear NMR spectra. The outcome of these reactions is summarized in Scheme 1.

Scheme 1



The reaction of $GaCl_3$ and $InCl_3$ with **4** yielded complexes **8** and **9** (Scheme 1) in low isolated yields (**8** and **12%**, respectively), presumably owing to partial decomposition of the ligand (loss of Te).¹⁷ The indium derivative **9** is considerably less prone to decomposition than the gallium analogue **8**, and consequently, it was characterized by CHN analysis, mass spectrometry, and a single-crystal X-ray structure. The ${}^{31}P$ NMR spectra of **8** and **9** exhibit similar patterns comprised of three resonances in the regions of 77–78, -41 to -45 , and -133 to -135 ppm with approximate relative intensities of 1:1:2. On the basis of the high-field chemical shift and lack of ${}^{125}Te$ satellites, the resonance at 77–78 ppm is attributed to a P^{III} center that is no longer attached to tellurium. By contrast, the resonance at 41–45 ppm displays satellites consistent with one-bond ${}^{31}P-{}^{125}Te$ coupling (1235–1250 Hz), showing that this P center is still bonded to tellurium. In the case of **9** the resonances at 78.1 and -41.2 ppm both exhibit a well-resolved doublet with ${}^2J(P,P) = 3.4$ Hz, consistent with mutual coupling of inequivalent P environments in the same *cyclo*- P_2N_2 ligand. On the basis of its relative intensity, the

third resonance at -133 and -135 ppm in **8** and **9**, respectively, which also displays satellites ($^1J(\text{P},\text{Te}) = 1115$ and 1130 Hz), is attributed to the symmetrical dianionic ligand L^{2-} ($\text{E} = \text{Te}$). This conclusion is supported by the ^{31}P NMR chemical shifts from ca. -136 to -141 ppm observed for the group 14 derivatives **10** and **12a–c** (vide infra). In summary, the ^{31}P NMR spectra for **8** and **9**, together with the CHN data and the observation of the molecular ion at $m/z = 1192.1$ in the mass spectrum of **9**, indicate that the M^{3+} center in these neutral complexes is symmetrically chelated to a dianionic ligand L^{2-} ($\text{E} = \text{Te}$) and also bonded to a monoanion in which the P_2N_2 platform is comprised of P^{III} and P^{V} centers.

Yellow platelets of the indium compound **9** were obtained by recrystallization from *n*-hexane, and the structure was determined by X-ray crystallography (Figure 1), which

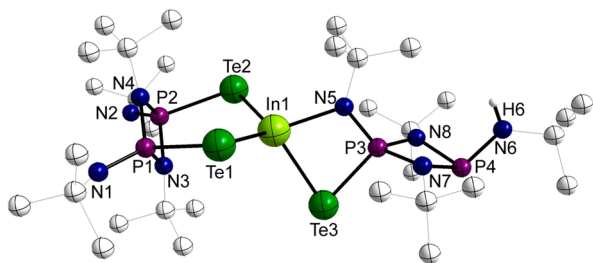


Figure 1. Molecular structure of **9**. Hydrogen atoms omitted for clarity. Selected bond lengths (Å) and angles (deg): Te1–In1 2.7270(16), Te1–P1 2.485(4), Te2–In1 2.7210(16), Te2–P2 2.499(3), Te3–In1 2.7959(6), Te3–P3 2.4526(10), In1–N5 2.174(3), P1–N1 1.559(12), P1–N3 1.699(13), P1–N4 1.662(12), P3–N5 1.610(4), P3–N7 1.644(11), P3–N8 1.686(11); In1–Te1–P1 93.37(8), In1–Te2–P2 93.05(8), In1–Te3–P3 71.40(3), Te1–In1–Te2 115.87(3), Te1–In1–Te3 114.25(6), Te1–In1–N5 113.4(4), Te2–In1–Te3 114.25(6), Te2–In1–N5 114.8(4), Te3–In1–N5 79.00(9).

confirmed the conclusions based on the ^{31}P NMR spectra. The spirocyclic structure of **9** is comprised of the dianionic ditelluro ligand L^{2-} ($\text{E} = \text{Te}$) coordinated to indium in a Te,Te'-mode and the Te,N-chelated monotelluro monoanion $[(^t\text{BuN}(\text{Te})\text{P}^{\text{V}}(\mu\text{-N}^t\text{Bu})_2\text{P}^{\text{III}}\text{N}(\text{H})^t\text{Bu})]^-$, which presumably results from the loss of tellurium from L^{2-} ($\text{E} = \text{Te}$) and monoprotonation.¹⁷

The mean P–Te distance of 2.492(4) Å for the ligand L^{2-} in **9** is comparable to that in the group 15 derivative [cf. 2.510(3) Å in **7b** ($\text{R} = \text{Ad}$)],¹⁶ while the third P–Te bond length of

2.453(1) Å is significantly shorter. The P–Te–In–Te–P scaffold was previously reported in the six-membered ring $\{\text{In}(\mu\text{-Te})[\text{N}(\text{Pr}_2\text{PTE})_2]\}_3$.¹⁸ The In–Te_{exo} distance of 2.809(1) Å in the latter complex¹⁸ is elongated when compared to the In–Te distances from the dianionic ligand L^{2-} in **9** (2.721(2)–2.727(2) Å), but comparable to the value of 2.796(1) Å observed for the Te3–In1 distance involving the monoanionic ligand.

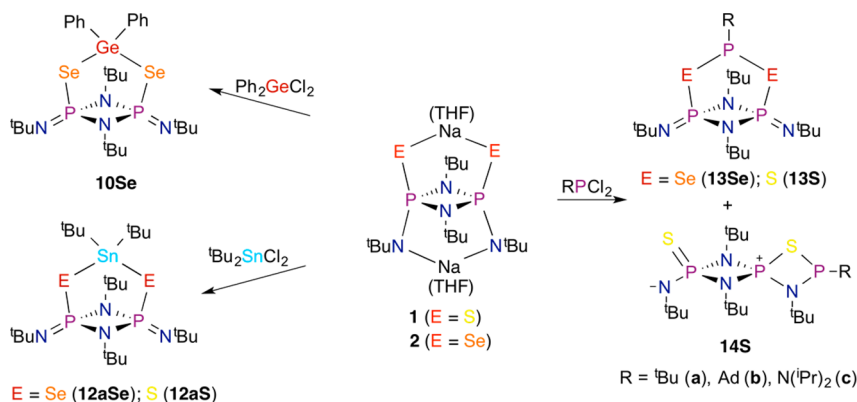
Synthesis, NMR Spectra, and Crystal Structures of Ph₂Ge Complexes. The reaction of **4** with Ph_2GeCl_2 produces the diphenylgermanium derivative **10** in 39% isolated yield (Scheme 1); no decomposition was observed in the solid state after 3 d of exposure to moist air. By contrast, the formation of the selenium analogue **10Se** (Scheme 2) was accompanied by the diprotonated derivative H_2L ($\text{E} = \text{Se}$) (**11Se**), which precluded the isolation of pure **10Se** due to their similar solubilities.¹⁹

The CHN analysis and the observation of the molecular ion in the high-resolution mass spectrum are consistent with the formation of the expected metathesis product **10**; furthermore, the singlet at -136.4 ppm ($^1J(\text{P},\text{Te}) = 1103$ Hz) strongly suggests symmetrical coordination of the ligand L^{2-} ($\text{E} = \text{Te}$) to the group 14 center. Yellow platelets of **10** were isolated from a saturated *n*-hexane solution stored at -40 °C, and an X-ray structural determination confirmed the Te,Te' coordination of the ligand to the Ph_2Ge unit (Figure 2).

The P–Te–E–Te–P ($\text{E} = \text{Ge}$) framework has not been previously reported, although a few examples of structurally characterized compounds incorporating Te–Ge–Te units were described. The mean Te–Ge bond distance in **10** is 2.571(3) Å, cf. 2.585(1)–2.600(1) Å in $[(2,4,6\text{-}^i\text{Pr}_3\text{C}_6\text{H}_2)_2\text{GeTe}_2]_2$ and 2.580(1) Å in $[(2,4,6\text{-}^i\text{Pr}_3\text{C}_6\text{H}_2)_4\text{Ge}_4\text{Te}_6]$.²⁰ The Ge atom is located 0.60 Å out of the mean Te1–P1–N1–N2–P2–Te2 plane in **10**, and the P_2N_2 ring is exactly perpendicular to this plane (Figure 2). The angle at the bridging Ge atom ($\angle\text{Te–Ge–Te}$) is $115.44(10)^\circ$, cf. $\angle\text{Te–Te–Te} = 104.50(1)^\circ$ in the cyclic tritelluride **6**¹⁴ and $\angle\text{Te–P–Te} = 108.81(16)^\circ$ in **7b**.¹⁶

The mass spectrum of the selenium analogue **10Se** shows a molecular ion at $m/z = 733.1$ [M^+H] with a characteristic isotopic pattern. The ^{31}P NMR spectrum consists of a singlet at -80.4 ppm accompanied by a set of satellites revealing $^1J(\text{P},\text{Se}) = 470$ Hz and $^2J(\text{P},\text{P}) = 60$ Hz. Consistently, the ^{77}Se NMR spectrum is comprised of a doublet of doublets centered at 137.6 ppm with $^1J(\text{P},\text{Se}) = 470$ Hz and $^3J(\text{P},\text{Se}) = 15.6$ Hz. Thus, the NMR data indicate symmetrical coordination of L^{2-} ($\text{E} = \text{Se}$) to the GePh_2 unit. Although yellow crystals of **10Se**

Scheme 2



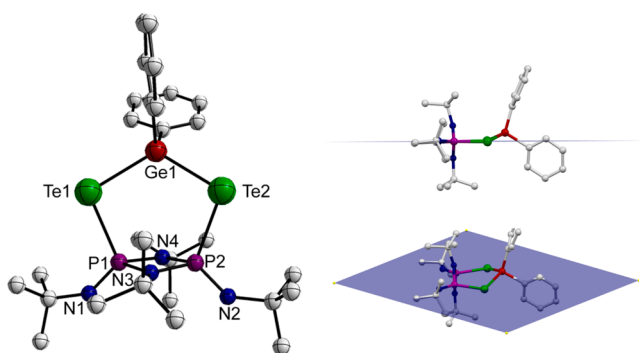


Figure 2. Molecular structure and side view of **10**. Hydrogen atoms omitted for clarity. Selected bond lengths (Å) and angles (deg): Te1–Ge1 2.577(3), Te2–Ge1 2.565(3), Te1–P1 2.508(6), Te2–P2 2.508(6), P1–N1 1.525(17), P1–N3 1.715(18), P1–N4 1.686(17), P2–N3 1.733(17), P2–N2 1.521(16), P2–N4 1.693(18); Ge1–Te1–P1 97.73(14), Ge1–Te2–P2 98.56(14), Te1–Ge1–Te2 115.44(10), Te1–P1–N1 114.0(7), Te1–P1–N3 107.1(7), Te1–P1–N4 109.3(6), Te2–P2–N3 108.5(7), Te2–P2–N2 115.6(7), Te2–P2–N4 107.2(6), N1–P1–N3 120.3(10), N1–P1–N4 117.9(10), N3–P1–N4 84.5(9).

were isolated, they were not of sufficient quality for the crystal structure to be determined.

Synthesis, NMR Spectra, and Crystal Structures of R_2Sn Complexes. Metathetical reactions of **4** with R_2SnCl_2 ($R = {}^tBu, {}^nBu, Ph$) were performed to evaluate the influence of the R group on the stability of the products. The air-sensitivity of the R_2Sn complexes **12a–c** varies dramatically; the tBu_2Sn derivative **12a** does not deteriorate upon exposure to air in the solid state for 3 d, whereas the nBu_2Sn (**12b**) and Ph_2Sn (**12c**) analogues decompose instantly with the formation of elemental tellurium (especially in solution), which precluded characterization by elemental analysis and mass spectrometry.

The Te,Te'-chelated structure of **12a** was established by an X-ray crystal structure (vide infra), and that arrangement is maintained in solution according to the NMR data (Table 1).

Table 1. Comparison of NMR Parameters for 12a–c, 12aSe, and 12aS^a

compound	12a	12b	12c	12aSe	12aS
E	Te	Te	Te	Se	S
R	^t Bu	ⁿ Bu	Ph	^t Bu	^t Bu
$\delta(^{31}P)$	–141.6	–140.4	–141.1	–77.0	–48.7
$^1J(^{31}P,E)^c$	1183	1102	1140	500	
$^2J(^{31}P,^{119}Sn)$	52	60	51	42	35
$\delta(^{119}Sn)$	34.2 (t)	–156.1 (t)	–84.7 (t)	69.8 (t)	66.4 (t)
$^1J(^{119}Sn,E)^c$	3385	<i>b</i>	3389	691	
$\delta(^{125}Te)$	–47.7 (dd)	23.4 (dd)	6.7 (dd)		
$\delta(^{77}Se)$				77.3 (dd)	
$^3J(^{31}P,E)^c$	25	26	26	12	

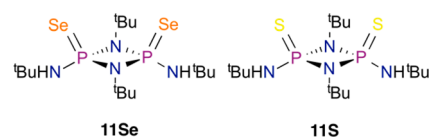
^a δ in ppm and J in Hz; t = triplet, dd = doublet of doublets. ^bPoor signal-to-noise ratios in the ^{119}Sn and ^{125}Te NMR spectra. ^cE = ^{77}Se or ^{125}Te .

Accordingly, the ^{31}P NMR spectrum exhibits a singlet accompanied by a doublet of tellurium satellites resulting from the magnetic inequivalence of the phosphorus centers [$^1J(P,Te) = 1183$ Hz and $^2J(P,P) = 3.4$ Hz]. Furthermore, tin satellites corresponding to $^2J(P,Sn) = 52$ Hz are observed. Consistently, the ^{119}Sn NMR spectrum exhibits a triplet

attributed to coupling to two equivalent phosphorus centers with satellites showing $^1J(Sn,Te) \approx 3390$ Hz. The ^{125}Te NMR spectrum consists of a doublet of doublets attributed to the $^1J(Te,P)$ and $^3J(Te,P)$ couplings. In addition, satellites confirming the $^1J(Te,Sn)$ value from the ^{119}Sn NMR spectra are apparent. Comparison of the NMR data for **12b** and **12c** with those of **12a** strongly suggest a similar framework, that is, Te,Te' chelation, for this series of R_2Sn ($R = {}^nBu, Ph, {}^tBu$) derivatives (Table 1).

To assess the influence of the chalcogen on the stability of R_2Sn derivatives of the dianions L^{2-} ($A = Te, Se, S$), the reactions of **1** and **2** with tBu_2SnCl_2 were also conducted. Although the ^{31}P NMR spectra indicated high yields of **12aS** and **12aSe** in solution (ca. 80%), and analytically pure crystals were obtained, the isolation of large amounts of these products was thwarted by the coformation of **11Se** and **11S**¹⁹ (Chart 3).

Chart 3



The ^{31}P NMR spectrum of **12aSe** exhibits a singlet at -77.0 ppm with two sets of satellites, $^1J(P,Se) = 500$ Hz and $^2J(P,Sn) = 42$ Hz. Similar to the observations for the tellurium analogue **12a**, the ^{119}Sn NMR spectrum of **12aSe** shows a triplet at 69.8 ppm ($^1J(Sn,Se) = 691$ Hz) and the ^{77}Se NMR spectrum exhibits a doublet of doublets at 77.3 ppm, which arises from the $^1J(P,Se)$ and $^3J(P,Se)$ couplings (Table 1). For comparison, the ^{31}P NMR spectrum of the tin(IV) complex $[Sn\{(Se)C(PPh_2Se)_2\}_2]$ shows a singlet at 61.6 ppm with $^1J(P,Se) = 536$ Hz²¹ and the tin(II) complex $[Sn\{NSeP^iPr_2\}_2Se,Se']_2$ exhibits a singlet at 58.8 ppm with $^1J(P,Se) = 550$ Hz and a $^2J(P,Sn) = 55$ Hz.²² The ^{31}P NMR spectrum of **12aS** consists of a single resonance at -48.7 ppm accompanied by ^{119}Sn satellites ($^2J(P,Sn) = 35$ Hz) and the ^{119}Sn NMR spectrum reveals a triplet at 66.4 ppm confirming the $^2J(P,Sn)$ values observed in the ^{31}P NMR spectrum (Table 1). Yellow (**12a**) and colorless crystals (**12aSe**, **12aS**) suitable for X-ray analysis were isolated after recrystallization from *n*-hexane at -40 °C. The molecular structures are illustrated in Figure 3, and structural parameters are compared in Table 2.

The structural determinations confirm the E,E' coordination of the ligands L^{2-} ($E = S, Se, Te$) to the group 14 center in all three derivatives. Interestingly, a N,N'-chelated isomer of **12aS** was characterized previously for Me_2SnL ($E = S$).²³ In that case, however, the isomer formed was predetermined by the synthetic approach, which involved oxidation of the two P^{III} centers in the N,N'-chelated complex $[({}^tBuNP^{III}(\mu-N^tBu)_2P^{III}N^tBu)(SnMe_2)]$ with sulfur.²³

In contrast to the observations for the Ph_2Ge derivative **10**, the $-P-Te-Sn-Te-P-$ framework is perfectly planar in **12a**, **12aSe**, and **12aS**; the P_2N_2 ring is perpendicular to that plane. The Sn–Te bond distance of 2.7603(7) Å in **12a** is comparable to the typical range (2.73–2.76 Å) reported for five-membered rings of the type $(R_2Sn)_3Te_2$ ($R = {}^tBu, {}^{24a}Fc^{24b}$). Although this bond is expectedly 0.19 and 0.32 Å longer than the corresponding distance in **12aSe** and **12aS**, the E–Sn–E bond angle varies by $<1.0^\circ$ in all three derivatives. Concomitantly, the P–E–Sn bond angle increases in the series $Te < Se < S$ from 100.7(1)° to 104.3(2)° consistent with higher

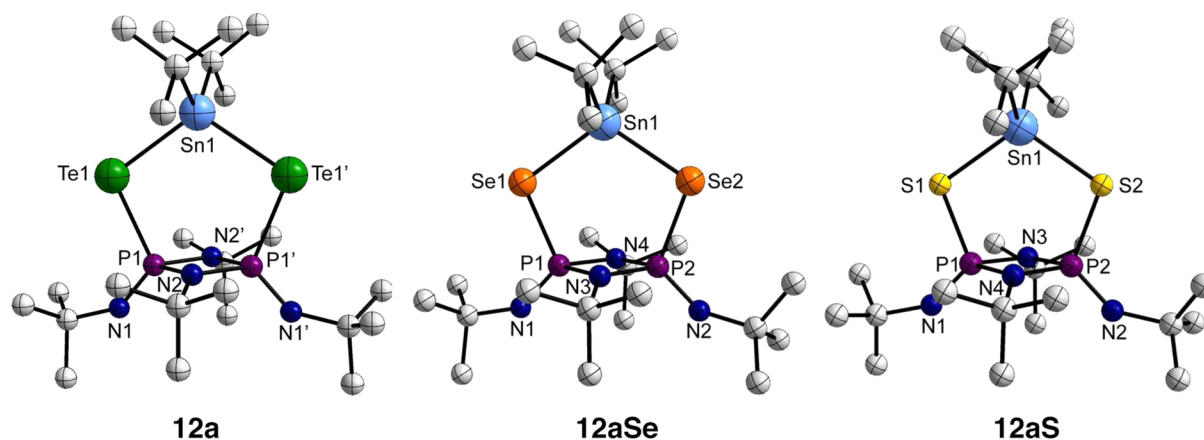


Figure 3. Molecular Structures of 12a, 12aSe, and 12aS.

Table 2. Comparison of Structural Data for 12a, 12aSe, and 12aS^a

compound	12a	12aSe	12aS
$d(\text{P}-\text{E})$	2.504(2)	2.277(3), 2.286(3)	2.110(4), 2.121(4)
$d(\text{E}-\text{Sn})$	2.7603(7)	2.5687(13), 2.5750(14)	2.444(4), 2.450(4)
$d(\text{P}-\text{N}_{\text{exo}})$	1.508(7)	1.521(10), 1.507(9)	1.484(10), 1.499(10)
$d(\text{P}-\text{N}_{\text{endo}})$	1.696(7), 1.693(7)	1.715(9), 1.693(9), 1.689(9), 1.698(9)	1.704(10), 1.696(9), 1.702(9), 1.702(10)
$d(\text{P}\cdots\text{Sn})$	4.056	3.808	3.603
$\angle\text{P}-\text{E}-\text{Sn}$	100.74(6)	102.73(8), 103.00(8)	104.34(17), 104.31(17)
$\angle\text{E}-\text{Sn}-\text{E}$	110.84(3)	110.35(4)	109.94(9)
$\angle\text{E}-\text{P}-\text{P}$	113.87(7)	112.45(13)	110.98(15)
$\angle\text{P}-\text{N}_{\text{endo}}-\text{P}$	96.2(4)	95.8(5), 95.4(5)	95.4(4), 95.1(4)
$\angle\text{E}-\text{P}-\text{N}_{\text{exo}}$	115.4(3)	114.3(4), 116.1(4)	115.5(4), 116.9(5)
$\angle\text{E}-\text{P}-\text{N}_{\text{endo}}$	107.3(3)	107.2(3), 107.4(3), 106.4(3), 106.7(3)	105.7(3), 107.4(3), 105.1(3), 107.1(3)

^aBond lengths in Å; bond angles in deg.

p-character in the chalcogen bonds for tellurium. The P–Te distance in **12a** is similar to that in **10**.

The structural motif P–Se–Sn–Se–P has been described in the octahedral Sn^{IV} compound $[\text{Sn}\{(\text{Se})\text{C}(\text{PPh}_2\text{Se})_2\}_2]^{21}$ and in the Sn^{II} complex $[\text{Sn}\{\text{NSeP}^i\text{Pr}_2\}_2\text{Se,Se}'\}_2]^{22}$. The P–Se distances of 2.277(3) and 2.286(3) Å in **12aSe** are in the typical single-bond range for P–Se rings.^{25,26} The P–S–Sn–S–P scaffold is well-known, for example, in diorganotin dithiophosphates $\text{Me}_2\text{Sn}(\text{S}_2\text{PR}_2)_2$ (R = Et,²⁷ Ph,²⁸ Me²⁹). The P–S bond distances in **12aS** are slightly longer (by ca. 0.10 Å) than the

mean value in diorganotin dithiophosphates, whereas the Sn–S bond lengths are marginally shorter (by 0.02–0.03 Å).

Synthesis and NMR Spectra of Organophosphorus Derivatives. In view of our recent synthesis of thermally stable organophosphorus(III)–tellurium heterocycles **7a** and **7b** via metathesis,^{15b} we have now investigated the reactions of **1** and **2** with $\text{R}(\text{PCl}_2)_2$ (R = ^tBu, Ad, ⁱPr₂N) to determine the influence of the chalcogen on the nature of the products. As indicated in Scheme 2, the Se,Se'-coordinated derivatives **13aSe** and **13bSe** are formed for the selenium system in yields of ca. 40% and 79%, respectively, on the basis of integrated ³¹P NMR spectra. In both cases colorless crystals were isolated, and the CHN analysis of **13aSe** was consistent with the molecular formula LP^tBu (E = Se); the symmetrical Se,Se'-coordination to the ^tBuP group was confirmed by a well-modeled disordered crystal structure (see Supporting Information).

The NMR spectra of **13aSe** and **13bSe** exhibit patterns similar to those of the tellurium analogues **7a** and **7b**.¹⁶ The ³¹P and ⁷⁷Se NMR spectra for the adamantyl derivative **13bSe**, as a representative example, are discussed here (Figure 4). The ³¹P NMR resonance at 132.0 ppm accompanied by ⁷⁷Se satellites (¹J(P,Se) = 232 Hz) is assigned to the P^{III} center in the bridging SePSe unit. The second resonance at –76.8 ppm shows a doublet of satellites with ¹J(P,Se) = 449 Hz and ²J(P,P) = 58 Hz, as expected for the chemically equivalent, but magnetically inequivalent, phosphorus atoms of the P₂N₂ ring. The large difference in ¹J(P,Se) values reflects the different formal oxidation states of the P^{III} and P^V environments. The ⁷⁷Se NMR spectrum of **13bSe** consists of a doublet of doublets centered at 226.5 ppm, which result from the two

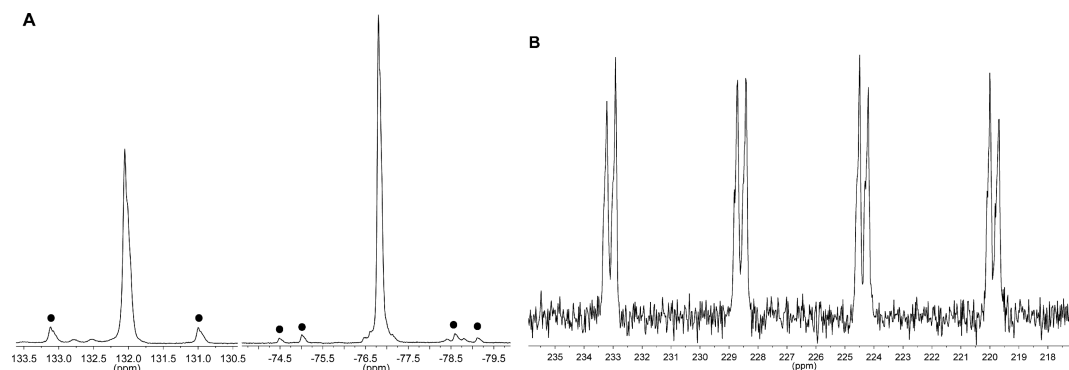


Figure 4. (A) ³¹P NMR and (B) ⁷⁷Se NMR spectra of **13bSe**.

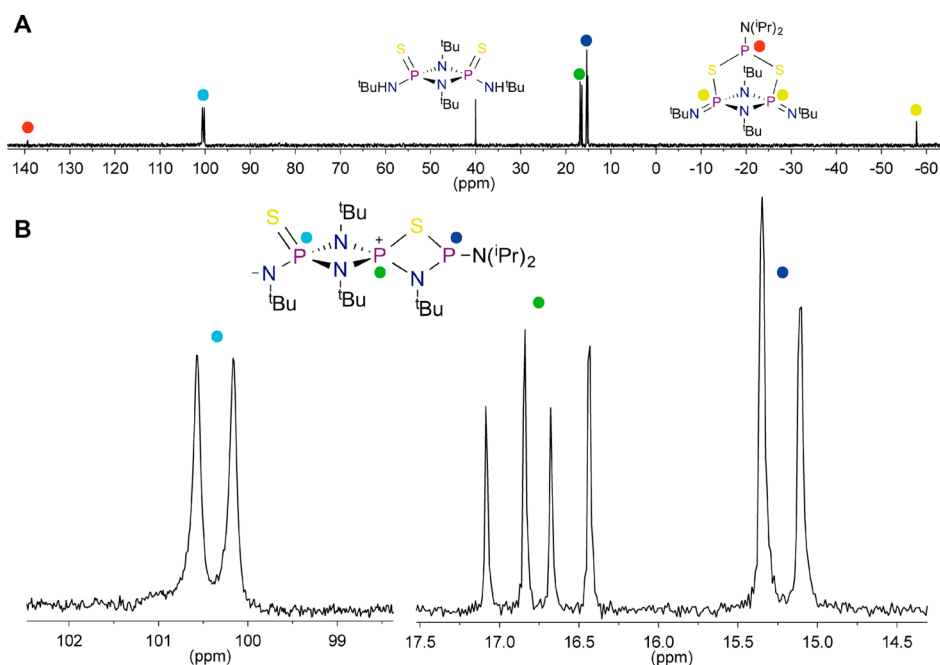


Figure 5. ^{31}P NMR spectrum of the reaction of **1** with $^1\text{Pr}_2\text{NPCl}_2$. (A) Complete spectrum. (B) Expanded spectrum for the N,S-chelated complex **14cS**.

aforementioned $^1\text{J}(\text{P},\text{Se})$ couplings and a $^3\text{J}(\text{Se},\text{P})$ coupling of 15.6 Hz (Figure 4).

In distinct contrast to the selenium and tellurium systems, the S,S'-chelated complexes **13a-cS** were formed in very low (<5%) yields, according to ^{31}P NMR spectra. Instead, the major products from the metathesis of **1** with R^+PCl_2 were the N,S-chelated complexes **14a-cS** (Scheme 2). The characterization of these products was based on the observation of the parent ion in the electrospray ionization (ESI) mass spectra and a detailed analysis of the ^{31}P NMR spectra. As a typical example, Figure 5A depicts the ^{31}P NMR spectrum of the reaction of **4** with $^1\text{Pr}_2\text{NPCl}_2$, which produces **14cS** as the major product, **13cS** as a very minor product, and **11S**. The ^{31}P NMR spectrum of the S,S'-chelated isomer **13cS** exhibits a mutually coupled 1:2:1 triplet and a doublet, attributed to the P^{III} (139.4 ppm) and P^{V} (-57.7 ppm) centers, respectively, with a small $^2\text{J}(\text{P},\text{P})$ coupling of 4.3 Hz that was not resolved in the case of the Se analogues **13aSe** and **13bSe**.

The expanded ^{31}P NMR spectrum of **14cS** (Figure 5B) reveals three distinct phosphorus environments resulting from the N,S-chelation of the ligand L^{2-} (E = S) to the RP^{III} center to give a zwitterion (Scheme 2). On the basis of the chemical shifts and coupling patterns, the three resonances can be assigned as follows: (a) a doublet at 100.4 ppm ($^2\text{J}(\text{P},\text{P}) = 44$ Hz) for the terminal P^{V} center, (b) a doublet of doublets at 16.8 ppm ($^2\text{J}(\text{P}^{\text{V}},\text{P}^{\text{V}}) = 45$ Hz, $^2\text{J}(\text{P}^{\text{V}},\text{P}^{\text{III}}) = 26$ Hz) for the spirocyclic P^{V} environment, and (c) a doublet at 15.2 ppm ($^2\text{J}(\text{P}^{\text{III}},\text{P}^{\text{V}}) = 26$ Hz) for the terminal P^{III} atom. The anomalous chemical shift for the spirocyclic P^{V} center is tentatively attributed to the formal positive charge on this atom in the zwitterionic structure of **14cS**. The NMR spectroscopic parameters for the adamantyl (**14bS**) and *tert*-butyl (**14aS**) derivatives, which show similar patterns, are summarized in Table 3.

The observation of different coordination modes of the ligands L^{2-} toward an RP^{2+} unit was unexpected; the only previous examples of N,S-chelation of the dianion L^{2-} (E = S)

Table 3. ^{31}P NMR Chemical Shifts and $^2\text{J}(\text{P},\text{P})$ for **14a-c^a**

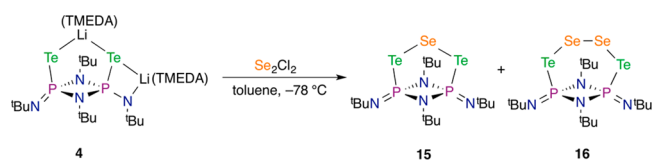
compound	14aS	14bS	14cS
$\delta(^{31}\text{P})$ ($\text{P}^{\text{V}}=\text{S}$)	116.9 (d)	111.4 (d)	100.4 (d)
$\delta(^{31}\text{P})$ (spirocyclic P^{V})	17.2 (dd)	17.3 (dd)	16.8 (dd)
$\delta(^{31}\text{P})$ (P^{III})	14.4 (d)	14.6 (d)	15.2 (d)
$^2\text{J}(\text{P}^{\text{V}},\text{P}^{\text{III}})$	27	27	26
$^2\text{J}(\text{P}^{\text{V}},\text{P}^{\text{V}})$	42	43	44

^a δ in ppm and J in Hz; d = doublet; dd = doublet of doublets.

were found in the tetrahydrofuran (THF)-solvated dilithium¹⁰ and dimethylaluminum derivatives.¹¹ The preferential formation of N,E-chelated organophosphorus(III) complexes for sulfur, but E,E'-bonded isomers for selenium and tellurium, may result from a combination of (a) the different bite angles of the two possible modes of chelation and (b) the higher stability of the zwitterionic structure **14S** (Scheme 2) for sulfur.

Synthesis, NMR Spectra, and Crystal Structures of Group 16 Complexes. Our previous syntheses of the cyclic tetraselenide **3**¹² and the cyclic tritelluride **6**,¹⁵ via metathesis, led us to consider whether this approach could be used as a source of mixed chalcogenido systems. Accordingly, the ditelluro reagent **4** was treated with Se_2Cl_2 in toluene at -78 °C. This reaction gave a complicated mixture of products, as revealed by ^{31}P NMR spectroscopy. The main components were cyclic derivatives **15** and **16** with Se^{2+} or $(\text{Se}-\text{Se})^{2+}$ units bridging the ligand L^{2-} (E = Te), respectively (Scheme 3); the former was the major product. In addition to the characterization of these mixed chalcogenides by multinuclear (^{31}P , ^{77}Se ,

Scheme 3



^{125}Te) NMR spectra, the X-ray structure of a single crystal of **16** was determined.

The molecular structure of **16** is illustrated in Figure 6 together with selected structural parameters. The tetrachalco-

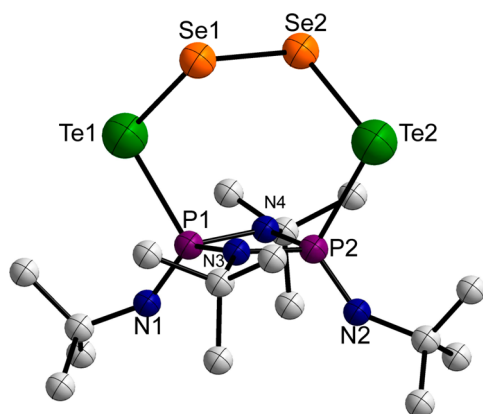


Figure 6. Molecular structure of **16**. Hydrogen atoms omitted for clarity. Selected bond lengths (Å) and angles (deg): Te1–Se1 2.4919(18), Te1–P1 2.483(3), Te2–Se2 2.5356(17), Te2–P2 2.501(3), Se1–Se2 2.391(2), P1–N1 1.502(10), P1–N3 1.688(9), P1–N4 1.701(9); Se1–Te1–P1 104.20(8), Se2–Te2–P2 101.64(8), Te1–Se1–Se2 102.88(7), Te2–Se2–Se1 101.47(7), Te1–P1–N1 113.3(4), Te1–P1–N3 108.1(3), Te1–P1–N4 107.7(3), N1–P1–N3 122.5(5), N1–P1–N4 117.7(5), N3–P1–N4 83.5(5).

genide **16** is the first example of a structurally characterized P–Te–Se–Se–Te–P arrangement. The Te–Se–Se–Te unit was described previously by Sladky et al. in the acyclic tetrachalcogenide TsiTeSeSeTeTsi (Tsi = C(SiMe₃)₃), but the solid-state structure was not determined;³⁰ it is also present in the cationic mixed-chalcogen clusters [Te₂Se₈]²⁺ and [Te₂Se₆]²⁺.³¹ The Te–Se distances of 2.492(2) and 2.536(2) Å and the Se–Se bond of 2.391(2) Å in **16** are comparable to the values reported for heterocycles in which a trichalcogenido unit bridges a benzene ring, d(Se–Te) = 2.523(1)–2.531(1) Å and d(Se–Se) = 2.350(1) Å.³² The P–Te bond lengths in **16** are similar to those in **6**.

Figure 7 compares the ring conformations of the two trichalcogenides **6**¹⁵ and **15**^{15a} and the two tetrachalcogenides

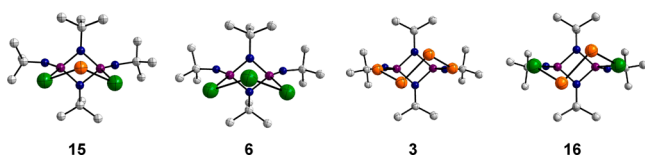


Figure 7. Conformations of *cyclo*-P₂N₂-supported polychalcogenides; Te atoms are shown in green, and Se atoms are in orange.

3¹² and **16**, all of which are supported by *cyclo*-P₂N₂ scaffolds. The extent of puckering is clearly very similar for the two trichalcogenides and the two tetrachalcogenides.

As indicated in Table 4, the previously reported NMR data for the tetraselenide **3**¹² and tritelluride **6**^{15a} provide an informative comparison for the assignment of the signals in the multinuclear NMR spectra of **15** and **16**. The resonance at –121.0 ppm in the ³¹P NMR spectrum of the TeSeTe-bridged derivative **15** appears as a singlet accompanied by both ¹²⁵Te and ⁷⁷Se satellites, ¹J(P,Te) = 1025 Hz and ²J(P,Se) = 29 Hz, cf. –134.5 ppm and ¹J(P,Te) = 1029 Hz for **6**.^{15a} The ⁷⁷Se

Table 4. Structural and NMR Parameters for *cyclo*-P₂N₂-Supported Polychalcogenides^{a,b}

	Te1Se3Te2 15	Te1Te3Te2 6	Se1Se3Se4Se2 3	Te1Se3Se4Te2 ^c 16
<i>d</i> (P1–E1)		2.5317(10)	2.280(3)	2.483(3)
<i>d</i> (P2–E2)		2.5405(10)	2.275(3)	2.501(3)
<i>d</i> (E1–E3)		2.7155(4)	2.3371(19)	2.4919(18)
δ (³¹ P)	–121.0	–134.5	–50.8	–68.6
¹ J(P,E)	1025	1029	524	1287
² J(P,E)	29	34	10	14
δ (⁷⁷ Se)	240.9 (t)		673.0 (t) 336.7 (dd)	465.6 (t)
δ (¹²⁵ Te)	870.3 (dd)	442.8 (dd) 361.9 (t)		711.6 (dd)

^aBond lengths in Å. ^b δ in ppm; *J* values in Hz; t = triplet, dd = doublet of doublets. ^cThe atomic numbering scheme is different from that in Figure 7 to compare analogous bond lengths in the tri- and tetrachalcogenide systems.

NMR spectrum of **15** reveals a 1:2:1 triplet at 240.9 ppm (²J(P,Se) = 29 Hz), and the ¹²⁵Te NMR spectrum shows a resonance at 870.3 ppm appearing as a doublet of doublets (¹J(P,Te) = 1025 Hz and ³J(Te,P) = 34 Hz).

The chemical shift of –68.6 ppm observed in the ³¹P NMR spectrum of the TeSeSeTe-bridged derivative **16** is close to the value of –50.8 ppm reported for the tetraselenide **3**,¹² cf. –121.0 ppm for **15**. Thus, it appears that ring conformation has a stronger influence than a change of chalcogens (Se vs Te) on the chemical shift in these examples. The ¹J(P,Te) value of 1287 Hz for **16** is substantially larger than the value of 1029 Hz found for the tritelluride **6**,^{15a} which is consistent with the shorter P–Te distance in **16** (Table 4).³³ The ⁷⁷Se NMR spectrum exhibits a triplet at 465.6 ppm (²J(P,Se) = 14 Hz), which can be compared with the triplet observed for the central Se atoms in the tetraselenide **3** at 673.0 ppm (²J(P,Se) = 10 Hz).¹² The ¹²⁵Te NMR spectrum of **16** confirms the P–Te coupling observed in the ³¹P NMR spectrum by showing a doublet of doublets at 711.6 ppm (¹J(P,Te) = 1289 Hz and ³J(P,Te) = 42 Hz).

The homoleptic tellurium(II) complex [Te{^tBu(H)N(Se)-P^V(μ -N^tBu)₂P^V(Se)^tBuN-N,Se₂}] (**17**) was identified as a minor product from the reaction of **4** with Se₂Cl₂,^{34,35} a small amount of the cyclic tritelluride **6** was also detected in the ³¹P NMR spectrum.

CONCLUSIONS

The thermal and air stability of main-group derivatives of the ditelluro dianion L^{2–} (E = Te) is markedly dependent on both the p-block element in the bridging position and the nature of the organyl groups in that linker. Thus, the Ph₂Ge and ^tBu₂Sn derivatives can be handled in air for several days, whereas other R₂Sn (R = ⁿBu, Ph) complexes decompose instantly with the formation of elemental tellurium.³⁶ The lability of the P–Te bond in the ligand L^{2–} was also evident in the reactions with MCl₃ (M = Ga, In) to give spirocyclic complexes in which one of the ligands incorporates a P^{III} center.

The Ph₂Ge derivative of the diseleno dianion L^{2–} (E = Se) is considerably more hydrolytically sensitive than the tellurium analogue; however, the complete series (L)Sn^tBu₂ (E = S, Se, Te) could be isolated enabling a structural comparison to be

Table 5. Crystallographic Data for 9, 10, and 16

compound	9	10	16
empirical formula	C ₃₂ H ₇₃ InN ₈ P ₄ Te ₃	C ₂₈ H ₄₆ GeN ₄ P ₂ Te ₂	C ₁₆ H ₃₆ N ₄ P ₂ Se ₂ Te ₂
formula weight	1191.50	828.44	759.55
temperature (°C)	93	125	93
crystal color, habit	yellow platelet	yellow platelet	red prism
crystal dimensions (mm ³)	0.10 × 0.10 × 0.01	0.17 × 0.07 × 0.02	0.10 × 0.10 × 0.10
crystal system	monoclinic	triclinic	monoclinic
a (Å)	10.439(2)	9.3375(18)	15.707(5)
b (Å)	13.630(2)	11.603(2)	14.808(4)
c (Å)	17.005(3)	15.879(3)	11.549(3)
α (deg)	90.0000	87.895(6)	90.0000
β (deg)	99.789(4)	80.914(6)	94.354(7)
γ (deg)	90.0000	89.309(6)	90.0000
volume (Å ³)	2384.5(7)	1697.6(6)	2678.4(13)
space group	P2 ₁	P $\bar{1}$	P2 ₁ /c
Z value	2	2	4
D _{calc} (g/cm ³)	1.659	1.621	1.883
F ₀₀₀	1172.00	816.00	1448.00
μ (Mo Kα) (cm ⁻¹)	2.459	2.703	5.025
No. of reflections measured	32 486	13 435	15 644
R _{int}	0.0463	0.1364	0.0512
min. and max. transmissions	0.683, 0.954	0.480, 0.947	0.414, 0.605
reflection/parameter ratio	8507 (433)	5948 (334)	4845 (235)
residuals: R ₁ (I > 2.00σ(I))	0.0204	0.1284	0.0780
residuals: wR ₂ (all reflections)	0.0505	0.3008	0.2127
maximum peak in final diff. map (e ⁻ /Å ³)	0.49	2.430	4.980
minimum peak in final diff. map (e ⁻ /Å ³)	-0.38	-1.910	-2.570

made. Organophosphorus(III) complexes of L²⁻ (E = S, Se) evinced a significant structural difference. As in the previous work with L²⁻ (E = Te),^{15b} E,E'-chelated complexes were the major products for selenium, but the N,S-chelated isomers predominated for the sulfur systems. The formation of Se,Se'-chelated complexes with p-block elements contrasts with our recent studies of coinage metal complexes in which attempted metathetical reactions of L²⁻ (E = Se) with silver(I) or gold(I) halides produces macrocycles that incorporate the monoprotonated ligand HL⁻.³⁹

The comprehensive survey of the reactions of the *cyclo*-P₂N₂-supported dianion L²⁻ (E = Te) with p-block element halides in this and previous work¹⁵ provides a benchmark for future studies of transition-metal, lanthanide, and actinide complexes of this tellurium-centered ligand, which have not yet been investigated. By contrast, d- and f-block metal complexes of the closely related PNP-bridged ditelluro monoanion [TeP^VR₂NP^VR₂Te]⁻ (R = ⁱPr) have received extensive attention,^{40–44} especially with regard to the nature of f-element tellurium bonds⁴⁴ and their use as single-source precursors of semiconducting metal tellurides in the form of thin films or quantum dots.⁴⁵

EXPERIMENTAL SECTION

Reagents and General Procedures. All synthetic manipulations were performed under an atmosphere of dry argon using standard Schlenk-line techniques and/or a Saffron glovebox operating with argon unless otherwise stated. All glass apparatus was stored in a drying oven (120 °C) and flame-dried in vacuo (1 × 10⁻³ mbar) before use. Dry solvents were collected from an MBraun solvent purification system under a nitrogen atmosphere and stored in Schlenk flasks over 4 Å molecular sieves or were dried and purified using common procedures.⁴⁶ All chemicals were purchased from Sigma-Aldrich, ABCR, Acros Organics, and Strem Chemicals Inc. and were

used without further purification unless otherwise stated. The products were stored in a glovebox under argon atmosphere or argon-fluted Schlenk or J. Young tubes or flasks. The cooling bath temperature of -78 °C was attained by using an acetone/dry ice bath.

Spectroscopic Methods. NMR spectra were recorded using a JEOL DELTA EX 270, a Bruker Avance 360 spectrometer, a BRUKER Avance II 400 spectrometer, a BRUKER Avance 500, or a BRUKER Avance III 500 spectrometer. ¹H, ¹³C, ³¹P{¹H}, ⁷⁷Se{¹H}, ¹¹⁹Sn{¹H}, and ¹²⁵Te{¹H} NMR spectra were measured in deuterated solvents or using the reaction mixture and capillaries filled with C₆D₆ at 25 °C. Tetramethylsilane was used as an internal standard for ¹H and ¹³C NMR. 85% H₃PO₄ was employed as an external standard for ³¹P{¹H} NMR spectra, Ph₂Te₂ or Me₂Te for ¹²⁵Te{¹H} NMR spectra, and Me₂Se for ⁷⁷Se{¹H} NMR spectra as well as Me₄Sn for ¹¹⁹Sn{¹H} NMR spectra. All ⁷⁷Se{¹H}, ¹¹⁹Sn{¹H} NMR, ¹²⁵Te{¹H}, and ³¹P{¹H} NMR spectra are reported as ⁷⁷Se, ¹²⁵Te, ¹¹⁹Sn, and ³¹P NMR spectra. Chemical shifts (δ) are given in parts per million (ppm) relative to the solvent peaks.⁴⁷ Coupling constants (J) are given in Hertz (Hz).

Mass spectra were obtained on a Finnigan MAT 95 XP, an Agilent 5975C Inert XL GC/MSD, or a Thermofisher LTQ Orbitrap XL at the EPSRC UK National MS Facility, Swansea. Elemental analysis was performed at the Elemental Analysis Service of the London Metropolitan University (by Mr. S. Boyer).

X-ray Crystallography. Crystallographic data were collected by using a Rigaku SCXmini (Mercury2 CCD) or the St. Andrews robotic diffractometer⁴⁸ at -148(1) °C or a Rigaku Mo MM07 (dual port) high brilliance generator with Saturn 70 and Mercury CCD detectors, rotating anode/confocal optics, and two XStream LT accessories at -180(1) °C. The data for 9 and 12aSe were collected using a Rigaku FRX RA generator, Dectris P200 detector and Oxford cryostream low-temperature device. All data were collected with Mo Kα radiation (λ = 0.710 73 Å) and corrected for Lorentz and polarization effects. The data for all of the compounds were collected and processed using CrystalClear (Rigaku).⁴⁸

The crystal structures were solved using direct methods⁴⁹ or heavy-atom Patterson methods⁵⁰ and expanded using Fourier techniques.⁵¹ The non-hydrogen atoms were refined anisotropically, while hydrogen

Table 6. Crystallographic Data for 12a, 12aSe, and 12aS

compound	12a	12aSe	12aS
empirical formula	C ₂₄ H ₅₄ N ₄ P ₂ SnTe ₂	C ₂₄ H ₅₄ N ₄ P ₂ SnSe ₂	C ₂₄ H ₅₄ N ₄ P ₂ SnS ₂
formula weight	834.56	737.28	643.48
temperature (°C)	125	93	125
crystal color, habit	yellow platelet	colorless prism	colorless platelet
crystal dimensions (mm ³)	0.24 × 0.18 × 0.03	0.10 × 0.03 × 0.03	0.15 × 0.09 × 0.03
crystal system	orthorhombic	monoclinic	monoclinic
<i>a</i> (Å)	20.1157(12)	19.345(4)	11.243(3)
<i>b</i> (Å)	30.241(2)	15.089(3)	30.770(7)
<i>c</i> (Å)	11.5584(7)	11.430(3)	11.193(3)
α (deg)	90.0000	90.0000	90.0000
β (deg)	90.0000	90.608(4)	119.829(17)
γ (deg)	90.0000	90.0000	90.0000
volume (Å ³)	7031.2(8)	3336.2(13)	3359.2(14)
space group	<i>Fdd2</i>	<i>Cc</i>	<i>P2₁/c1</i>
Z value	8	4	4
<i>D</i> _{calc} (g/cm ³)	1.577	1.468	1.272
<i>F</i> ₀₀₀	3280.00	1496.00	1352.00
μ (Mo K α) (cm ⁻¹)	2.462	3.062	0.998
No. of reflections measured	14 705	21 515	25 146
<i>R</i> _{int}	0.0712	0.1101	0.1092
min. and max. transmissions	0.665, 0.929	0.515, 0.912	0.641, 0.971
reflection/parameter ratio	3097 (150)	5669 (316)	5901 (298)
residuals: <i>R</i> ₁ (<i>I</i> > 2.00 σ (<i>I</i>))	0.0373	0.0516	0.0840
residuals: <i>wR</i> ₂ (all reflections)	0.0748	0.1233	0.2759
maximum peak in final diff. map (e ⁻ /Å ³)	0.540	2.87	1.890
minimum peak in final diff. map (e ⁻ /Å ³)	-0.380	-2.00	-1.210

atoms were refined using the riding model. All calculations were performed using CrystalStructure⁵² crystallographic software package and SHELXL-97.⁵³ Despite several crystals being examined, thin plates of **10**, **12aS**, and **16** gave only average quality results, and hence only the main features of the structures are discussed above. Crystallographic data for **9**, **10**, **12a**, **12aSe**, **12aS**, and **16** are summarized in Tables 5 and 6.

General Procedure for Metathetical Reactions. The reagent **1**, **2**, **10**, **4**, **14** or **5**^{15a} (0.60 mmol) was suspended in toluene (10 mL) and cooled to -78 °C. A solution of the p-block element halide R_nMCl₂ (*n* = 1, 2) or MCl₃ (0.59 mmol) in toluene (10 mL) at -78 °C was added dropwise to the suspension of **1**, **2**, **4**, or **5** over 15 min by cannula. The reaction mixture was stirred at -78 °C for 2 h and then warmed to room temperature. After stirring for an additional 1 h, the precipitate (LiCl or NaCl) was removed by filtration, and the solvent was removed under vacuum. The obtained solid was dissolved in *n*-hexane and maintained at -40 °C overnight. The crystals were removed by filtration and dried under vacuum. The resulting filtrate was concentrated and cooled to -40 °C to produce another batch of crystals.

Synthesis of 8. Reagents: **4** (500 mg, 0.590 mmol) and GaCl₃ (53 mg, 0.30 mmol, 0.5 equiv) in toluene (20 mL). Red crystals of **8** were isolated from *n*-hexane (yield 8%). ³¹P NMR (202.46 MHz, [D₈]toluene): δ = 76.6 (s), -44.7 (s, ¹J(P,Te) = 1233 Hz), -133.3 (s, ¹J(P,Te) = 1130 Hz, ³J(P,Te) = 184 Hz). Decomposition in toluene or THF precluded the acquisition of a ¹²⁵Te NMR spectrum.

Synthesis of 9. Reagents: InCl₃ (66 mg, 0.30 mmol, 0.5 equiv) (179 mg, 0.590 mmol) and **4** (500 mg, 0.590 mmol) in toluene (20 mL). Recrystallization from *n*-hexane afforded yellow crystals suitable for X-ray crystallography (yield 12%). ³¹P NMR (109.37 MHz, [D₈]toluene): δ = 78.1 (d, ²J(P,P) = 3.4 Hz), -41.2 (d, ¹J(P,Te) = 1251 Hz, ²J(P,P) = 3.4 Hz), -135.1 (s, ¹J(P,Te) = 1113 Hz, ²J(P,P) = 10.2 Hz). Decomposition during the measurement precluded reliable characterization by ¹²⁵Te NMR. MS (EI⁺), *m/z*, 1192.1 (M⁺), 1177.1 (M⁺-CH₃). Anal. Calcd (%) for C₃₂H₇₃N₈P₄InTe₃: C 32.26, H 6.18, N 9.40; found: C 32.32, H 6.20, N 9.59.

Synthesis of 10. Reagents: **4** (500 mg, 0.590 mmol) and Ph₂GeCl₂ (176 mg, 0.590 mmol) in toluene (20 mL). Yield of red crystals = 39%. ¹H NMR (400.13 MHz, [D₈]toluene): δ = 7.78–7.75 (m, 4H, Ph), 7.12–7.05 (m, 6H, Ph), 1.57 (s, 18H, *t*Bu), 1.39 (s, 18H, *t*Bu). ³¹P NMR (161.98 MHz, [D₈]toluene): δ = -136.4 (s, ¹J(P,Te) = 1103 Hz, ²J(P,P) = 20 Hz). ¹²⁵Te NMR (85.24 MHz, [D₈]toluene): δ = 162.4 (¹J(P,Te) = 1105 Hz, ³J(P,Te) = 26 Hz). HRMS (EI): *m/z* Found: 834.0528 (M⁺), Calcd for C₂₈H₄₆N₄⁷⁴GeP₂¹³⁰Te₂ 834.0528. Anal. Calcd (%) for C₂₈H₄₆GeN₄P₂Te₃: C 40.59, H 5.80, N 6.76; found: C 40.65, H 5.65, N 6.84.

Synthesis of 10Se. Reagents: **2** (500 mg, 0.600 mmol, 1 equiv) and Ph₂GeCl₂ (178 mg, 0.600 mmol) in toluene (25 mL). Yellow prismatic crystals were obtained from *n*-hexane solution at -78 °C. ³¹P NMR (109.37 MHz, [D₈]THF): δ = -80.4 (¹J(P,Se) = 470.3 Hz, ²J(P,P) = 60.2 Hz). ⁷⁷Se NMR (51.52 MHz, [D₈]THF): δ = 137.6 (dd, ¹J(Se,P) = 470.1 Hz, ³J(Se,P) = 15.6 Hz). MS (EI⁺): *m/z* 733.1 (M⁺+H), calcd: 733.1.

Synthesis of 12a. Reagents: ¹Bu₂SnCl₂ (179 mg, 0.590 mmol) and **4** (500 mg, 0.590 mmol) in toluene (25 mL). Yellow crystals of **12a** isolated in 34% yield. ¹H NMR (270.17 MHz, [D₈]toluene): δ = 1.71 (s, 18H, ¹Bu) 1.46 (s, 18H, ¹Bu), 1.38 (s, 18H, ¹Bu). ³¹P NMR (109.37 MHz, [D₈]toluene): δ = -141.6 (s, ¹J(P,Te) = 1183 Hz, ²J(P,Sn) = 52 Hz, ²J(P,P) = 6.1 Hz). ¹¹⁹Sn NMR (100.75 MHz, [D₈]toluene): δ = 34.2 (²J(P,Sn) = 52 Hz, ¹J(Sn,Te) = 3385 Hz). ¹²⁵Te NMR (85.24 MHz, [D₈]toluene): δ = -47.7 (¹J(P,Te) = 1181 Hz, ³J(P,Te) = 25 Hz). MS (EI), *m/z*: 836.2 (M⁺), calcd: 836.1; 821.1 [M⁺-CH₃], calcd: 821.1. HRMS (EI), *m/z*: 783.0260 [M⁺-*t*Bu], calcd for C₂₀H₄₅N₄P₂Sn₁Te₂: 783.0260. Elemental analysis calcd (%) for C₂₄H₅₄N₄P₂SnTe₂: C 34.54, H 6.52, N 6.71; found: C 34.45, H 6.57, N 6.62.

Synthesis of 12b. Reagents: ¹Bu₂SnCl₂ (179 mg, 0.590 mmol) and **1** (500 mg, 0.590 mmol) in toluene (25 mL). Yellow crystals were isolated, but characterization was limited to NMR spectra owing to their extremely air-sensitive nature. ¹H NMR (270.17 MHz, [D₈]toluene): δ = 1.71 (s, 18H, ¹Bu), 1.66–1.47 (m, 4H+4H, ¹Bu), 1.44 (s, 18H, ¹Bu), 1.32 (s, 4H, ²J(HH) = 7.6 Hz, ¹Bu), 0.90 (t, 6H, ²J(HH) = 7.6 Hz, ¹Bu). ³¹P NMR (202.46 MHz, [D₈]toluene): δ =

−141.1 (s, $^1J(\text{P},\text{Te}) = 1140$ Hz, $^2J(\text{P},\text{Sn}) = 51$ Hz). ^{119}Sn NMR (100.75 MHz, $[\text{D}_8]\text{toluene}$): $\delta = -84.7$ ($^2J(\text{P},\text{Sn}) = 52$ Hz, $^1J(\text{Sn},\text{Te}) = 3288$ Hz). ^{125}Te NMR (85.24 MHz, $[\text{D}_8]\text{toluene}$): $\delta = 6.7$ (dd, $^1J(\text{P},\text{Te}) = 1137$ Hz, $^3J(\text{P},\text{Te}) = 26$ Hz).

Synthesis of 12c. Reagents: Ph_2SnCl_2 (203 mg, 0.590 mmol) and **4** (500 mg, 0.590 mmol) in toluene (25 mL). Yellow crystals were isolated, but characterization was limited to NMR spectra owing to their extremely air-sensitive nature. ^{31}P NMR (161.98 MHz, $[\text{D}_8]\text{toluene}$): $\delta = -140.4$ (s, $^1J(\text{P},\text{Te}) = 1102$ Hz, $^2J(\text{P},\text{Sn}) = 60$ Hz, $^2J(\text{P},\text{P}) = 6.5$ Hz). ^{119}Sn NMR (100.75 MHz, $[\text{D}_8]\text{toluene}$): $\delta = -156.1$ ($^2J(\text{P},\text{Sn}) = 62$ Hz). ^{125}Te NMR (85.24 MHz, $[\text{D}_8]\text{toluene}$): $\delta = 23.4$ ($^1J(\text{P},\text{Te}) = 1102$ Hz, $^3J(\text{P},\text{Te}) = 26$ Hz).

Synthesis of 12aSe. Reagents: **2** (500 mg, 0.600 mmol) and $^t\text{Bu}_2\text{SnCl}_2$ (182 mg, 0.600 mmol) in toluene (15 mL). Yield of **12aSe** = 78% according to the ^{31}P NMR spectrum; yellow crystals were isolated. ^{31}P NMR (109.37 MHz, $[\text{D}_8]\text{THF}$): $\delta = -77.0$ (s, $^1J(\text{P},\text{Se}) = 500.0$ Hz, $^2J(\text{P},\text{Sn}) = 42.3$ Hz). ^{119}Sn NMR (100.75 MHz, $[\text{D}_8]\text{THF}$): $\delta = 69.8$ ($^2J(\text{P},\text{Sn}) = 43.1$ Hz, $^1J(\text{Sn},\text{Se}) = 690.5$ Hz). ^{77}Se NMR (51.52 MHz, $[\text{D}_8]\text{THF}$): $\delta = 77.3$ ($^1J(\text{P},\text{Se}) = 498.2$ Hz, $^3J(\text{P},\text{Se}) = 12.0$ Hz). EIMS, m/z : 723.1 ($\text{M}^+ - \text{CH}_3$), calcd 723.1. Anal. Calcd (%) for $\text{C}_{24}\text{H}_{34}\text{N}_4\text{P}_2\text{SnSe}_2$: C 39.10, H 7.38, N 7.60; found: C 39.06, H 7.40, N 7.56.

Synthesis of 12aS. Reagents: **1** (500 mg, 0.680 mmol) and $^t\text{Bu}_2\text{SnCl}_2$ (207 mg, 0.680 mmol) in toluene (25 mL). Yield of **12aS** = 80% according to the ^{31}P NMR spectrum; colorless crystals were isolated. ^{31}P NMR (109.37 MHz, $[\text{D}_8]\text{toluene}$): $\delta = -48.7$ (s, $^2J(\text{P},\text{Sn}) = 35.2$ Hz). ^{119}Sn NMR (100.75 MHz, $[\text{D}_8]\text{THF}$): $\delta = 66.4$ ($^2J(\text{P},\text{Sn}) = 33.9$ Hz). EIMS, m/z : 629.2 ($\text{M}^+ - \text{CH}_3$), calcd 629.2. Anal. Calcd (%) for $\text{C}_{24}\text{H}_{34}\text{N}_4\text{P}_2\text{SnS}_2$: C 44.80, H 8.46, N 8.71; found: C 44.73, H 8.49, N 8.80.

Synthesis of 13aSe. Reagents $^t\text{BuPCl}_2$ (95 mg, 0.60 mmol) and **2** (500 mg, 0.590 mmol) in toluene (25 mL). Estimated yields from the ^{31}P NMR spectrum were **13aSe** (40%) and **11Se** (20%), which cocrystallized as colorless crystals. ^{31}P NMR data for **13aSe**: ^{31}P NMR (109.37 MHz, $[\text{D}_8]\text{THF}$): $\delta = 139.5$ ($^1J(\text{P},\text{Se}) = 234.1$ Hz), -78.0 ($^1J(\text{P},\text{Se}) = 447.3$ Hz, $^2J(\text{P},\text{P}) = 58.0$ Hz). ^{77}Se NMR (51.52 MHz, $[\text{D}_8]\text{THF}$): $\delta = 256.0$ ($^1J(\text{Se},\text{P}^{\text{IV}}) = 450.8$ Hz, $^1J(\text{Se},\text{P}^{\text{III}}) = 234.4$ Hz, $^3J(\text{Se},\text{P}) = 19.6$ Hz). EIMS, m/z : 580.1 ($\text{M}^+ - \text{CH}_3 + \text{H}$), calcd 580.1. A few crystals of pure **13aSe** were isolated. Anal. Calcd (%) for $\text{C}_{20}\text{H}_{45}\text{N}_4\text{P}_3\text{Se}_2$: C 40.55, H 7.66, N 9.46; found: C 40.71, H 7.77, N 9.37.

Synthesis of 13bSe. Reagents: AdPCl_2 (214 mg, 0.600 mmol) and **2** (500 mg, 0.590 mmol) in toluene (25 mL). Yield of **13bSe** estimated from integration of the ^{31}P NMR spectrum ca. 79% **13bSe** formed colorless cocrystals with the byproduct **11Se**. ^{31}P NMR data for **13bSe**: ^{31}P NMR (109.37 MHz, $[\text{D}_8]\text{THF}$): $\delta = 132.0$ ($^1J(\text{P},\text{Se}) = 231.8$ Hz), -76.8 ($^1J(\text{P},\text{Se}) = 449.5$ Hz, $^2J(\text{P},\text{P}) = 58.0$ Hz). ^{77}Se NMR (51.52 MHz, $[\text{D}_8]\text{THF}$): $\delta = 226.5$ (ddd, $^1J(\text{Se},\text{P}^{\text{V}}) = 449.0$ Hz, $^1J(\text{Se},\text{P}^{\text{III}}) = 232.1$ Hz, $^3J(\text{Se},\text{P}) = 15.6$ Hz).

Synthesis of 13aS and 14aS. Reagents: **1** (500 mg, 0.680 mmol) and $^t\text{BuPCl}_2$ (107 mg, 0.680 mmol) in toluene (25 mL). Estimated yield of **13aS** and **14aS** were ca. 5% and 67%, respectively, from the integrated ^{31}P NMR spectrum. ^{31}P NMR and MS data for **13aS**: ^{31}P NMR (109.37 MHz, C_6D_6 -capillary): $\delta = 126.5$ (s), -56.9 (s). EIMS, m/z : 498.2 (M^+), calcd 498.2; 483.1 ($\text{M}^+ - \text{CH}_3$), calcd 438.2. NMR and MS data for **14aS**: ^{31}P NMR (109.37 MHz, C_6D_6 -capillary): $\delta = 116.9$ (d, $^2J(\text{P},\text{P}) = 42.3$ Hz), 17.2 (dd, $^2J(\text{P},\text{P}) = 42.5$ Hz, $^2J(\text{P},\text{P}) = 27.1$ Hz), 14.4 (d, $^2J(\text{P},\text{P}) = 27.0$ Hz). EIMS, m/z : 498.2 (M^+), calcd 498.2; 483.1 ($\text{M}^+ - \text{CH}_3$), calcd 483.2.

Synthesis of 13bS and 14bS. Reagents: **1** (500 mg, 0.680 mmol) and AdPCl_2 (159 mg, 0.680 mmol, 1 equiv) in toluene (25 mL). Estimated yields of **13bS** and **14bS** were ca. 3% and 71%, respectively, from the integrated ^{31}P NMR spectrum. ^{31}P NMR and MS data for **13bS**: ^{31}P NMR (109.37 MHz, C_6D_6 -capillary): $\delta = 120.1$ (s), -56.2 (s). EIMS, m/z : 576.3 (M^+), calcd 576.3; 561.3 ($\text{M}^+ - \text{CH}_3$), calcd 561.3. NMR and MS data for **14bS**: ^{31}P NMR (109.37 MHz, C_6D_6 -capillary): $\delta = 111.4$ (d, $^2J(\text{P},\text{P}) = 43.4$ Hz), 17.3 (dd, $^2J(\text{P},\text{P}) = 43.4$ Hz, $^2J(\text{P},\text{P}) = 26.9$ Hz), 14.6 (d, $^2J(\text{P},\text{P}) = 26.8$ Hz). EIMS, m/z : 576.3 (M^+), calcd 576.3; 561.3 ($\text{M}^+ - \text{CH}_3$), calcd 561.3.

Synthesis of 13cS and 14cS. Reagents: **1** (500 mg, 0.680 mmol) and $(^i\text{Pr})_2\text{NPCL}_2$ (159 mg, 0.680 mmol) in toluene (25 mL). Estimated yields of **13cS** and **14cS** were ca. 2% and 93%, respectively, from the integrated ^{31}P NMR spectrum. ^{31}P NMR and MS data for **13cS**: ^{31}P NMR (109.37 MHz, C_6D_6 -capillary): $\delta = 139.4$ (t, $^2J(\text{P},\text{P}) = 4.3$ Hz), -57.7 (d, $^2J(\text{P},\text{P}) = 4.3$ Hz). EIMS, m/z : 541.3 (M^+), calcd 541.3 (M^+); 526.2 ($\text{M}^+ - \text{CH}_3$), calcd 526.2. NMR and MS data for **14cS**: ^{31}P NMR (109.37 MHz, $[\text{D}_8]\text{THF}$): $\delta = 100.4$ (d, $^2J(\text{P},\text{P}) = 44.4$ Hz), 16.8 (dd, $^2J(\text{P},\text{P}) = 44.6$ Hz, $^2J(\text{P},\text{P}) = 25.9$ Hz), 15.2 (d, $^2J(\text{P},\text{P}) = 26.2$ Hz). EIMS, m/z : 541.3 (M^+), calcd 541.3 [$\text{M}^+ - \text{H}$]; 526.2 ($\text{M}^+ - \text{CH}_3$), calcd 526.2.

Synthesis of 15 and 16. Reagents: Se_2Cl_2 (135 mg, 0.590 mmol) and **1** (500 mg, 0.590 mmol) in toluene (25 mL). NMR data for the major product **15**: ^{31}P NMR (109.37 MHz, $[\text{D}_8]\text{toluene}$): $\delta = -121.0$ ($^1J(\text{P},^{125}\text{Te}) = 1025$ Hz; $^2J(\text{P},^{77}\text{Se}) = 29$ Hz; $^2J(\text{P},\text{P}) = 23$ Hz). ^{77}Se NMR (51.52 MHz, $[\text{D}_8]\text{toluene}$): $\delta = 240.9$ (t, $^2J(\text{P},^{77}\text{Se}) = 30$ Hz) ppm. ^{125}Te NMR (85.24 MHz, $[\text{D}_8]\text{toluene}$): δ [ppm] = 870.3 (dd, $^1J(\text{P},^{125}\text{Te}) = 1025$ Hz; $^3J(\text{P},^{125}\text{Te}) = 34$ Hz). NMR data for **16**: ^{31}P NMR (109.37 MHz, $[\text{D}_8]\text{toluene}$): $\delta = -68.6$ ($^1J(\text{P},^{125}\text{Te}) = 1287$ Hz; $^2J(\text{P},\text{P}) = 47$ Hz; $^1J(\text{P},^{77}\text{Se}) = 14$ Hz) ppm. ^{77}Se NMR (51.52 MHz, $[\text{D}_8]\text{toluene}$): $\delta = 465.6$ (pseudo-t, $^2J(\text{P},^{77}\text{Se}) = 14$ Hz). ^{125}Te NMR (85.24 MHz, $[\text{D}_8]\text{toluene}$): $\delta = 711.6$ (dd, $^1J(\text{P},^{125}\text{Te}) = 1289$ Hz; $^3J(\text{P},^{125}\text{Te}) = 42$ Hz). A few red crystals of **16** were isolated; Anal. Calcd (%) for $\text{C}_{16}\text{H}_{36}\text{N}_4\text{P}_2\text{Te}_2\text{Se}_2$: C 25.30, H 4.78, N 7.38; found: C 25.32, H 4.92, N 7.47.

The cyclic tritelluride **6** was identified as a byproduct in the ^{31}P and ^{125}Te NMR spectra. ^{31}P NMR (109.37 MHz, $[\text{D}_8]\text{toluene}$): $\delta = -134.6$ ($^1J(\text{P},^{125}\text{Te}) = 1028$ Hz; $^2J(\text{P},\text{P}) = 31$ Hz). ^{125}Te NMR (126.43 MHz, $[\text{D}_8]\text{toluene}$): $\delta = 442.8$ (dd, $^1J(\text{P},\text{Te}) = 1031$ Hz, $^3J(\text{P},\text{Te}) = 41$ Hz), 361.9 (t, $^1J(^{125}\text{Te},^{123}\text{Te}) = 1254$ Hz, $^2J(\text{P},\text{Te}) = 35$ Hz).

■ ASSOCIATED CONTENT

📄 Supporting Information

X-ray crystallographic files in CIF format for compounds **9**, **10**, **12a**, **13aSe**, **12b**, **12c**, **16**, and **18Se**. Synthesis of **18**, **18Se**, **18S**, and **19**. X-ray crystallography, featuring structural drawings of **13aSe** and **18Se**. Additional references. This material is available free of charge via the Internet at <http://pubs.acs.org>.

■ AUTHOR INFORMATION

Corresponding Author

*E-mail: chivers@ucalgary.ca. Fax: (+1) 403-289-9488. Phone: (+1) 403-220-5741.

Notes

The authors declare no competing financial interest.

■ ACKNOWLEDGMENTS

The authors are grateful to the EPSRC, the EPSRC National Mass Spectrometry Service Centre (NMSSC) Swansea, the School of Chemistry St. Andrews, EaStCHEM, and NSERC Canada for financial support.

■ REFERENCES

- (1) Chivers, T.; Manners, I. *Inorganic Rings and Polymers of the p-Block Elements: From Fundamentals to Applications*; RSC Publishing: Cambridge, U.K., 2009; pp 231–236.
- (2) For reviews, see (a) Balakrishna, M. S.; Eisler, D. J.; Chivers, T. *Chem. Soc. Rev.* **2007**, *36*, 650. (b) Stahl, L. *Coord. Chem. Rev.* **2000**, *210*, 203. (c) Balakrishna, M. S.; Reddy, V. S.; Krishnamurthy, S. S.; Nixon, J. F.; Burckett St Laurent, J. C. T. R. *Coord. Chem. Rev.* **1994**, *129*, 1. (d) Keat, R. *Top. Curr. Chem.* **1982**, *102*, 89.
- (3) For a review, see Calera, S. G.; Wright, D. S. *Dalton Trans.* **2010**, *39*, S055 and references cited therein.
- (4) Balakrishna, M. S. *J. Organomet. Chem.* **2010**, *695*, 925.

- (5) Siddiqui, M. M.; Mobin, S. M.; Senkovska, I.; Kaskel, S.; Balakrishna, M. S. *Chem. Commun.* **2014**, *50*, 12273.
- (6) Garcia, F.; Goodman, J. M.; Kowenicki, R. A.; Kuzu, I.; McPartlin, M.; Silva, M. A.; Riera, L.; Woods, A. D.; Wright, D. S. *Chem.—Eur. J.* **2004**, *10*, 6066.
- (7) Chandrasekharan, P.; Mague, J. T.; Balakrishna, M. S. *Dalton Trans.* **2009**, 5478.
- (8) Briand, G. G.; Chivers, T.; Krahn, M. *Coord. Chem. Rev.* **2002**, *233–234*, 237 and references cited therein.
- (9) Chivers, T.; Krahn, M.; Parvez, M. *Chem. Commun.* **2000**, 463.
- (10) Chivers, T.; Krahn, M.; Parvez, M.; Schatte, G. *Inorg. Chem.* **2001**, *40*, 2547.
- (11) Lief, G. R.; Carrow, C. J.; Stahl, L. *Organometallics* **2001**, *20*, 1629.
- (12) Nordheider, A.; Chivers, T.; Thirumoorthi, R.; Vargas-Baca, I.; Woollins, J. D. *Chem. Commun.* **2012**, *48*, 6346.
- (13) For a review of main group derivatives of the P^{III}/P^{III} dianion [tBuNP^{III}(μ-N^tBu)]₂²⁻ see Stahl, L. *Coord. Chem. Rev.* **2000**, *210*, 203.
- (14) Briand, G. G.; Chivers, T.; Parvez, M. *Angew. Chem., Int. Ed.* **2002**, *41*, 3468.
- (15) (a) Nordheider, A.; Chivers, T.; Thirumoorthi, R.; Athukorala Arachchige, K. S.; Slawin, A. M. Z.; Woollins, J. D.; Vargas-Baca, I. *Dalton Trans.* **2013**, *42*, 3291. (b) Nordheider, A.; Chivers, T.; Schön, O.; Karaghiosoff, K.; Athukorala Arachchige, K. S.; Slawin, A. M. Z.; Woollins, J. D. *Chem.—Eur. J.* **2014**, *20*, 704.
- (16) Hinz, A.; Kuzora, R.; Rosenthal, U.; Schulz, A.; Villinger, A. *Chem.—Eur. J.* **2014**, *45*, 14659.
- (17) The lability of the P–Te bond, especially in the presence of organolithium reagents, is common feature of phosphorus(V)-tellurium chemistry that gives rise to low yields. For recent examples, see (a) Daniliuc, C.; Druckenbrodt, C.; Hrib, C. G.; Ruthe, F.; Blaschette, A.; Jones, P. G.; du Mont, W.-W. *Chem. Commun.* **2007**, 2060. (b) Ritch, J. S.; Chivers, T. *Dalton Trans.* **2008**, 957. (c) Konu, J.; Tuononen, H. M.; Chivers, T. *Inorg. Chem.* **2009**, *48*, 11788. (d) Elder, P. J. W.; Chivers, T.; Thirumoorthi, R. *Eur. J. Inorg. Chem.* **2013**, 2867. (e) Jeremias, L.; Babiak, M.; Kubát, V.; Calhorda, M. J.; Trávníček, Z.; Novosad, J. *RSC Adv.* **2014**, *4*, 15428.
- (18) Copsey, M. C.; Chivers, T. *Chem. Commun.* **2005**, 4938.
- (19) In a previous investigation the formation of **11Se** ($\delta(^{31}\text{P}) = 26.7$ ppm, $^1\text{J}(\text{P,Se}) = 880$ Hz) and **11S** ($\delta(^{31}\text{P}) = 40.0$ ppm) was proposed to be the result of a radical process. Semi-empirical MO calculations of the model system [Me(H)N(S)P^V(μ-NMe)₂P^V(S)NMe]⁺ indicated a nitrogen-based SOMO (spin population at nitrogen = 0.957) in preference to the formation of a sulfur-based radical. Such nitrogen-based radicals will abstract hydrogen atoms from the solvent to form **11S** (or **11Se**). This prediction was supported by the detection of a N-centered radical intermediate by EPR spectra in the reaction of Li[tBuN(S)P^V(μ-N^tBu)₂P^V(S)N(H)^tBu] with TeCl₄, which produces **11S** as one of the products. Briand, G. G.; Chivers, T.; Schatte, G. *Inorg. Chem.* **2002**, *41*, 1958.
- (20) Ramaker, G.; Saak, W.; Haase, D.; Weidenbruch, M. *Organometallics* **2003**, *22*, 5212.
- (21) Konu, J.; Chivers, T. *Chem. Commun.* **2010**, 46, 1431.
- (22) Rufino-Felipe, E.; Osorio, E.; Merino, G.; Muñoz-Hernández, M.-A. *Dalton Trans.* **2013**, *42*, 11180.
- (23) Linti, G.; Nöth, H.; Schneider, E.; Storch, W. *Chem. Ber.* **1993**, *126*, 611.
- (24) (a) Puff, H.; Breuer, B.; Schuh, W.; Sievers, R.; Zimmer, R. *J. Organomet. Chem.* **1987**, *332*, 279. (b) You, Z.; Bergunde, J.; Gerke, B.; Pöttgen, R.; Dehnen, S. *Inorg. Chem.* **2014**, *53*, 12512.
- (25) Bhattacharyya, P.; Slawin, A. M. Z.; Woollins, J. D. *J. Chem. Soc., Dalton Trans.* **2001**, 300.
- (26) Hua, G.; Li, Y.; Slawin, A. M. Z.; Woollins, J. D. *Angew. Chem., Int. Ed.* **2008**, *47*, 2857.
- (27) Silvestru, C.; Haiduc, I.; Klima, S.; Thewalt, U.; Gielen, M.; Zuckerman, J. J. *J. Organomet. Chem.* **1987**, *327*, 181.
- (28) Casas, J. S.; Castiñeiras, A.; Rodríguez-Argüelles, M. C.; Sánchez, A.; Sordo, J.; Vázquez-López, A.; Vázquez-López, E. M. *J. Chem. Soc., Dalton Trans.* **2000**, 4056.
- (29) Molloy, K. C.; Hossain, M. B.; van der Helm, D.; Zuckerman, J. J.; Mullins, F. P. *Inorg. Chem.* **1981**, *20*, 2172.
- (30) Sladky, F.; Bildstein, B.; Rieker, C.; Gieren, A.; Betz, H.; Hübner, T. *J. Chem. Soc., Chem. Commun.* **1985**, 1800.
- (31) Collins, M. J.; Gillespie, R. J.; Sawyer, J. F. *Inorg. Chem.* **1987**, *26*, 1476.
- (32) Ogawa, S.; Yoshimura, S.; Nagahora, N.; Kawai, Y.; Mikata, Y.; Sato, R. *Chem. Commun.* **2002**, 1918.
- (33) An inverse correlation between $d(\text{P–Te})$ and $^1\text{J}(\text{P,Te})$ values for cyclo-P₂N₂ derivatives with a terminal Te substituent has previously been discussed. Briand, G. G.; Chivers, T.; Parvez, M.; Schatte, G. *Inorg. Chem.* **2003**, *42*, 525.
- (34) The tellurium(II) complex [Te{tBu(H)N(Se)P^V(μ-N^tBu)₂P^V(Se)tBuN-N,Se}]₂ was previously prepared by the reaction of 2 equiv of the monoanion HL⁻ (E = Se) with TeCl₄, and the X-ray structure revealed bis-N,Se chelation. Briand, G. G.; Chivers, T.; Schatte, G. *Inorg. Chem.* **2002**, *41*, 1958.
- (35) In the current work the structure of the minor byproduct [Te{tBu(H)N(Se)P^V(μ-N^tBu)₂P^V(Se)tBuN-N,Se}]₂ was determined, and the structural parameters were similar to the reported values.³⁴ The formation of P^V–Se linkages in this reaction indicates significant decomposition of the ditelluro ligand L²⁻ (E = Te) (presumably, via Se–Te exchange). Further evidence of that process is provided by the detection of the neutral diselenido precursor **11Se** in the ³¹P NMR spectrum of the reaction mixture.
- (36) The reactions of **1**, **2**, and **4** with EtAsI₂ and PhSbCl₂, as representative examples of heavier group 15 elements, were also performed. Although the solution ³¹P NMR spectra were consistent with the formation of Te,Te'-chelated complexes of L²⁻, the lability of these derivatives (extrusion of Te) precluded further characterization (see Supporting Information).
- (37) (a) Separation of **10Se** from **11Se** ($\delta(^{31}\text{P}) = 26.7$ ppm, $^1\text{J}(\text{P,Se}) = 880$ Hz)¹⁰ was not possible due to their similar solubility. (b) Separation of **12aS** from **11S** ($\delta(^{31}\text{P}) = 40.0$; cf. lit. value 39 ppm (in [D₈]toluene) = 38.7)³⁸ was thwarted by their similar solubility..
- (38) Hill, T. G.; Haltiwanger, R. C.; Thompson, M. L.; Katz, S. A.; Norman, A. D. *Inorg. Chem.* **1994**, *33*, 1770.
- (39) Nordheider, A.; Hüll, K.; Athukorala Arachchige, K. S.; Slawin, A. M. Z.; Woollins, J. D.; Thirumoorthi, R.; Chivers, T. *Dalton Trans.* **2015**, DOI: 10.1039/c5dt00159e.
- (40) For a review, see Chivers, T.; Ritch, J. R.; Robertson, S. D.; Konu, J.; Tuononen, H. M. *Acc. Chem. Res.* **2010**, *43*, 1053.
- (41) Group 10: (a) Levesanos, N.; Robertson, S. D.; Maganas, D.; Raptopoulou, C. P.; Terzis, A.; Kyritsis, P.; Chivers, T. *Inorg. Chem.* **2008**, *47*, 2949. (b) Robertson, S. D.; Ritch, J. S.; Chivers, T. *Dalton Trans.* **2009**, 8582.
- (42) Group 11: (a) Copsey, M. C.; Panneerselvam, A.; Afzaal, M.; Chivers, T.; O'Brien, P. *Dalton Trans.* **2007**, 1528. (b) Eisler, D. J.; Robertson, S. D.; Chivers, T. *Can. J. Chem.* **2009**, *87*, 39.
- (43) Group 12: (a) Chivers, T.; Eisler, D. J.; Ritch, J. S. *Dalton Trans.* **2005**, 2675. (b) Garje, S. S.; Ritch, J. S.; Eisler, D. J.; Afzaal, M.; O'Brien, P.; Chivers, T. *J. Mater. Chem.* **2006**, *16*, 966.
- (44) Lanthanides and actinides: (a) Gaunt, A. J.; Scott, B. L.; Neu, M. P. *Angew. Chem., Int. Ed.* **2006**, *45*, 1638. (b) Ingram, K. I. M.; Kaltsoyannis, N.; Gaunt, A. J.; Neu, M. P. *J. Alloys Compd.* **2007**, *444–445*, 369. (c) Gaunt, A. J.; Reilly, S. D.; Enriquez, A. E.; Scott, B. L.; Ibers, J. A.; Sekar, P.; Ingram, K. I. M.; Kaltsoyannis, N.; Neu, M. P. *Inorg. Chem.* **2008**, *47*, 29. (d) Ingram, K. I. M.; Tassell, M. J.; Gaunt, A. J.; Kaltsoyannis, N. *Inorg. Chem.* **2008**, *47*, 7824.
- (45) Ritch, J. S.; Afzaal, M.; Chivers, T.; O'Brien, P. *Chem. Soc. Rev.* **2007**, *36*, 1622.
- (46) Perrin, D. D.; Armarego, W. L. F. *Purification of Laboratory Chemicals*, 6th ed.; Butterworth-Heinemann: Oxford, U.K., 2009.
- (47) Fulmer, G. R.; Miller, A. J. M.; Sherden, N. H.; Gottlieb, H. E.; Nudelman, A.; Stoltz, B. M. *Organometallics* **2010**, *29*, 2176.
- (48) (a) Fuller, A. L.; Scott-Hayward, L. A. S.; Li, Y.; Bühl, M.; Slawin, A. M. Z.; Woollins, J. D. *J. Am. Chem. Soc.* **2010**, *132*, 5799–5802. (b) *CrystalClear 2.0*; Rigaku Corporation: Texas, U.S., 2012. (c) Pflugrath, J. W. *Acta Crystallogr.* **1999**, *D55*, 1718.

(49) Altomare, A.; Burla, M.; Camalli, M.; Cascarano, G.; Giacovazzo, C.; Guagliardi, A.; Moliterni, A.; Polidori, G.; Spagna, R. *J. Appl. Crystallogr.* **1999**, *32*, 115.

(50) Beurskens, P. T.; Admiraal, G.; Behm, H.; Beurskens, G.; Smits, J. M. M.; Smykalla, C. *Z. Kristallogr.* **1991**, *Suppl. 4*, 99.

(51) Beurskens, P. T.; Admiraal, G.; Beurskens, G.; Bosman, W. P.; de Gelder, R.; Israel, R.; Smits, J. M. M. *The DIRDIF-99 program system*; Technical Report of the Crystallography Laboratory; University of Nijmegen: The Netherlands, 1999.

(52) (a) *CrystalStructure 3.8.1*: Crystal Structure Analysis Package; Rigaku and Rigaku/MSC, The Woodlands, TX, 2000–2006. (b) *CrystalStructure 4.0*: Crystal Structure Analysis Package; Rigaku Corporation: Tokyo, Japan, 2000–2010; pp 196–8666.

(53) Sheldrick, G. M. *Acta Crystallogr.* **2008**, *A64*, 112.